Guided-Wave Experiments with Dielectric Waveguides Having Finite Periodic Corrugation

MIKIO TSUJI, MEMBER, IEEE, SOICHI MATSUMOTO, STUDENT MEMBER, IEEE, HIROSHI SHIGESAWA, MEMBER, IEEE, AND KEI TAKIYAMA, MEMBER, IEEE

Abstract —**A planar dielectric waveguide having finite periodic rectangular corrugation is investigated analytically and experimentally, in case of surface waves propagating at an angle to the corrugation. In analytical considerations, a finitely corrugated guide is regarded as consisting of many step discontinuities connected by a length of uniform slab waveguide, and its propagation characteristics in the Bragg interaction region are derived from a cascaded connection of the transmission matrix expressing a step discontinuity. Although the present method takes only surface wave modes into account and neglects the wave with continuous spectrum, the calculated results show an excellent agreement with experimental ones which are performed for an *H*-guide in the microwave region.**

I. Introduction

The PERIODIC corrugations placed on top of dielectric waveguides are widely used in the millimeter-wave and optical-wave regions as filters, resonators, grating couplers, leaky wave antennas, and so on [1]. The analyses of such corrugations have been mainly performed by the approximate method [2]–[5], based on the coupled mode equations valid for small periodic perturbations, and also the more rigorous method [6], [7], based on the space harmonic expansion of waves according to the Floquet's theorem. However, these methods are essentially effective only for waveguides having infinite periodic corrugation. Seeing this fact from the viewpoint of practical component design, these methods give no necessary information about the effects of the length or the periodic number of corrugation, even if the boundary conditions relating to the finite length are introduced into the coupled mode equations as seen in [4].

One attractive approach to solving this problem has been presented by Rozzi *et al.* [8], [9]. They considered a wave propagating normal to the corrugation, and regarded the finite periodic corrugation as a cascade of the step discontinuities. They derived its characteristics from the accurate finite network description for such cascades.

More recently, unlike a surface wave propagating normal to the corrugation, the effects of a surface wave propagating at an angle to the corrugation are utilized in certain sophisticated components for integrated optics, e.g., the Bragg deflector [10] and the chirped-grating demultiplexer [11]. One can also encounter such an oblique propagation of millimeter waves in corrugated dielectric image guides with small dimensions comparable to the wavelength. In the case of oblique propagation, Peng and Oliner [12] have pointed out that it is necessary to consider the mode conversion between different polarizations, i.e., the coupling between TE and TM waves. Wagatsuma *et al.* [13] and Shiao *et al.* [14] have analyzed this problem by modifying slightly the coupled mode equations and by using the space harmonic expansion method, respectively. However, these methods again assume the infinite periodic structure as mentioned above. From the practical point of view, the analysis of finite periodic corrugation for oblique guidance seems to be more important. The application of Rozzi's method to this problem may be difficult because his method is effective only for a case in which a surface wave propagates normal to the corrugation.

Thus, in this paper, we present the approximate analytical method for planar dielectric waveguides with finite periodic corrugation in which the wave propagates at an angle to the corrugation. This method is based on the oblique incident problem of the surface wave onto the step discontinuity. The finite periodic corrugation is treated in a cascaded connection of the step discontinuities as seen in Rozzi's approach. When a corrugation is operated in the stopbands corresponding to the Bragg reflection, the structure of practical components may be chosen so that the unwanted radiation occuring at the step discontinuity may become small. Then, disregarding the interaction via the continuous spectrum, it may be expected that the present method treating only surface waves results in a good approximation for the propagation characteristics in the stopband regions. In fact, the scaled experiments which are performed by using the corrugated *H*-guide in the 10-GHz region will satisfactorily prove the usefulness of the present method.

II. Analysis

A. Transmission Matrix for the Step Discontinuity

As described in the previous section, it is necessary first to analyze a step discontinuity problem in which the surface wave mode is obliquely incident onto it. The discontinuity that we are concerned with here is depicted in Fig. 1. The

Manuscript received July 7, 1982; revised November 24, 1982.
The authors are with the Department of Electronics, Doshisha University, Kyoto, 602 Japan.

0018-9480/83/0400-0337$01.00 ©1983 IEEE

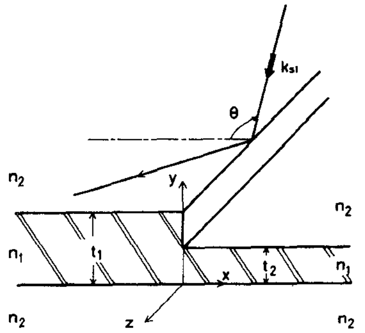

(a)

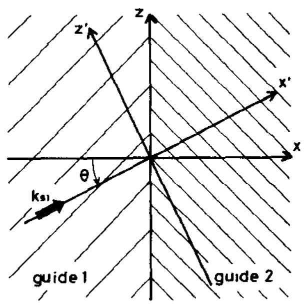

(b)

Fig. 1. (a) Pictorial representation of the step discontinuity in a dielectric slab waveguide, where the TE surface wave mode is incident obliquely to the step at an angle θ. (b) Its top view indicating relationship between the two coordinate systems.

slab guide 1, on the left-hand side, has the thickness t_1, and the slab guide 2, on the right-hand side, has the thickness t_2 ($< t_1$). For simplicity, it is assumed that both slab guides can support only the lowest TE and TM surface wave modes, and the negligible radiation occurs at a step discontinuity. The latter assumption may be valid when the thickness ratio t_1/t_2 is nearly equal to unity. Furthermore, the succeeding analysis will assume the oblique incidence of the TE surface wave mode at an angle θ onto the step discontinuity from the left-hand side of the structure as shown in Fig. 1(a).

Referring to [15], the fields of a TE and a TM surface wave modes in the (x, y, z) coordinates can be easily obtained by the coordinate transformation from the eigencoordinate system (x', y, z') in which the x' coordinate indicates the propagation direction of an incident surface wave mode as shown in Fig. 1(b). The fields in the (x, y, z) coordinates have five components ($E_y = 0$ for TE, $H_y = 0$ for TM), and the tangential components to the yz plane at $x = 0$ can be given in each guide as follows:

Guide 1

$$\begin{aligned}
E_{y1} &= C_R \frac{1}{n_1^2(y)} \bar{U}_1(y)\\
E_{z1} &= (1+R) Z_{x1} U_1(y) - C_R \frac{1}{n_1^2(y)} \bar{Y}_{z1} \bar{V}_1(y)\\
H_{y1} &= -(1-R) U_1(y)\\
H_{z1} &= -(1-R) Z_{z1} V_1(y) - C_R \bar{Y}_{x1} \bar{U}_1(y).
\end{aligned} \tag{1}$$

Guide 2

$$\begin{aligned}
E_{y2} &= C_T \frac{1}{n_2^2(y)} \bar{U}_2(y)\\
E_{z2} &= T Z_{x2} U_2(y) - C_T \frac{1}{n_2^2(y)} \bar{Y}_{z2} \bar{V}_2(y)\\
H_{y2} &= -T U_2(y)\\
H_{z2} &= -T Z_{x2} V_2(y) + C_T \bar{Y}_{x2} \bar{U}_2(y)
\end{aligned} \tag{2}$$

where

$$\begin{aligned}
&Z_{xi} = Z_{si} \cos\theta_i \quad Z_{zi} = Z_{si} \sin\theta_i \quad Z_{si} = \omega\mu_0 / k_{si}\\
&\bar{Y}_{xi} = \bar{Y}_{si} \cos\bar{\theta}_i \quad \bar{Y}_{zi} = \bar{Y}_{si} \sin\bar{\theta}_i \quad \bar{Y}_{si} = \omega\epsilon_0 / \bar{k}_{si}\\
&V_i = \frac{1}{j\omega\mu_0} \frac{\partial U_i}{\partial y} \quad \bar{V}_i = -\frac{1}{j\omega\epsilon_0} \frac{\partial \bar{U}_i}{\partial y}
\end{aligned} \tag{3}$$

and

$$n_i(y) = \begin{cases} n_2, & 0 \geqq y \geqq t_i \\ n_1, & 0 \leqq y \leqq t_i \qquad (i = 1,2). \end{cases} \tag{4}$$

In these expressions, the overbar is used to denote quantities for TM modes; $U_i(y)$ and $\bar{U}_i(y)$ are the normalized transverse modal functions (see, for example, [16, ch. 8.3]); k_{si} and $\bar{k}_{si}$ are the longitudinal propagation constants of surface modes in the slab guide. R and T denote the amplitude reflection and transmission coefficients of the incident TE mode, respectively, while C_R and C_T denote the amplitude coupling coefficients of the incident TE mode to the TM surface wave modes with the opposite polarization in guides 1 and 2, respectively.

It is noted that for the scattering problem under consideration here, the wavenumber k_z in the z direction is already known through the parameters k_{si} and θ of the incident TE mode, so that the angles of reflection and transmission for every TE or TM mode are determined through the following Snell's law:

$$k_z = k_{s1} \sin\theta_1 = k_{s2} \sin\theta_2 = \bar{k}_{s1} \sin\bar{\theta}_1 = \bar{k}_{s2} \sin\bar{\theta}_2. \tag{5}$$

This relation means that the magnitudes of unknown coefficients should be solved by taking these peculiar angles of propagation into account carefully. For this purpose, it is necessary to normalize the modal functions U_i and $\bar{U}_i$ in the following fashion:

$$Z_{xi}\langle U_i, U_i \rangle = \bar{Y}_{xi} \left\langle \bar{U}_i, \frac{\bar{U}_i}{n_i^2(y)} \right\rangle = 1 \qquad (i = 1,2) \tag{6}$$

where

$$\langle \phi_i, \psi_i \rangle = \int_{-\infty}^{\infty} \phi_i(y) \psi_i(y)\, dy. \tag{7}$$

Equation (6) demands the power flow along the x axis to be unity per unit width of z.

The unknown coefficients R, T, C_R, and C_T can be solved from the condition that the field components in the yz plane in both guides 1 and 2 must be continuous at the discontinuity plane at $x = 0$. After taking the inner product of each continuity condition of four tangential field components with U_1 or $\overline{U}_1$, and performing a number of algebraic procedures, the coefficients can be solved as follows:

$$
\begin{aligned}
\frac{1+R}{1-R} &= \frac{Z_{x2}}{Z_{x1}} + \zeta \overline{Y}_{z1}\left\langle V_1, \frac{\overline{U}_1}{n_1^2(y)} \right\rangle - \eta \overline{Y}_{z2}\left\langle U_1, \frac{\overline{V}_2}{n_2^2(y)} \right\rangle \\
T &= \frac{1-R}{Z_{x1}\langle U_1, U_2\rangle} \\
C_R &= \zeta(1-R) \\
C_T &= \eta(1-R)
\end{aligned} \tag{8}
$$

where

$$
\begin{aligned}
\eta &= \frac{1}{\overline{Y}_{x1}\left\langle \overline{U}_1, \dfrac{\overline{U}_2}{n_2^2(y)} \right\rangle + \overline{Y}_{x2}\left\langle \overline{U}_2, \dfrac{\overline{U}_1}{n_1^2(y)} \right\rangle} \\
&\quad \cdot \left\{ \frac{Z_{z2}}{Z_{x1}} \frac{\left\langle V_2, \dfrac{\overline{U}_1}{n_1^2(y)} \right\rangle}{\langle U_1, U_2\rangle} - Z_{z1}\left\langle V_1, \frac{\overline{U}_1}{n_1^2(y)} \right\rangle \right\} \\
\zeta &= \eta \overline{Y}_{x1}\left\langle \overline{U}_1, \frac{\overline{U}_2}{n_2^2(y)} \right\rangle.
\end{aligned} \tag{9}
$$

Next, let us express a step discontinuity in a transmission matrix by using these coefficients. For simplicity, we shall first derive a scattering matrix with 4×4 elements shown in Fig. 2. The incidence of the TE mode from the left-hand side corresponds to the situation that only the incident wave a_1 exists (i.e., $a_2 = a_3 = a_4 = 0$), and four elements of the scattering matrix $S_{m1}(m = 1,2,3,4)$ can be obtained as follows:

$$
\begin{aligned}
S_{11} &= R \quad S_{21} = C_R \\
S_{31} &= T \quad S_{41} = C_T.
\end{aligned} \tag{10}
$$

Following the same method, the other elements $S_{mn}(n = 1,2,3,4)$ of the scattering matrix can be obtained by considering the TM-mode incidence from guide 1 and also the incidence of each type mode from guide 2. Hereafter, for convenience sake, the transmission matrix will be used instead of the scattering matrix derived above.

B. Analysis of the Finite and Infinite Periodic Corrugations

As shown in Fig. 3, a periodic rectangular corrugation on the surface of a dielectric slab may be viewed as consisting of many step discontinuities connected by a length of uniform slab waveguide. The propagation characteristics for the periodic corrugation may be calculated by a cascaded connection of the transmission matrices of both the discontinuity and the uniform slab. Such an approximate approach is valid for the case when only the propagating surface waves are taken into account. This assumption will be followed throughout this paper. Now, denoting the transmission matrices of the nth discontinuity and the nth uniform slab by $\boldsymbol{T}_n$ and $\boldsymbol{T}_{l\cdot n}$, respectively, one

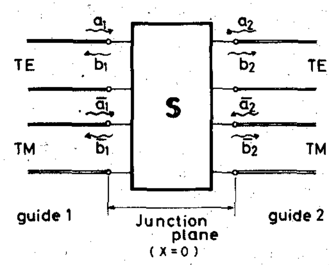

Fig. 2. Equivalent network for the step discontinuity.

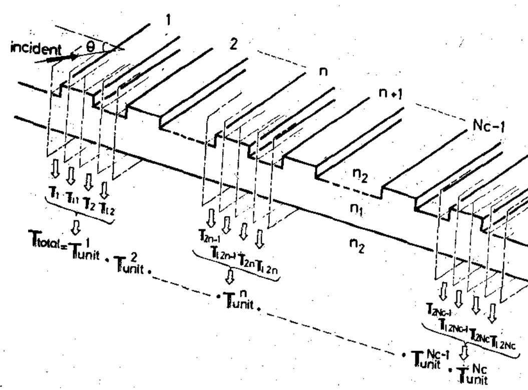

Fig. 3. Dielectric slab waveguide with finite periodic corrugation. T_{unit}^n means the transmission matrix of nth unit cell and the finite corrugation is expressed by the cascaded connection of T_{unit}^n $(n = 1,2,\cdots,N_c)$.

can define a unit cell or a building block constructed by $\boldsymbol{T}_{\text{unit}}^n = \boldsymbol{T}_{2n-1}\cdot \boldsymbol{T}_{l\cdot 2n-1}\cdot \boldsymbol{T}_{2n}\cdot \boldsymbol{T}_{l\cdot 2n}$ as shown in Fig. 3. Then the transmission matrix $\boldsymbol{T}_{\text{total}}$ for the finite periodic corrugation consisting of N_c unit cells can be given as follows:

$$
\boldsymbol{T}_{\text{total}} = \prod_{n=1}^{N_c} \boldsymbol{T}_{\text{unit}}^n. \tag{11}
$$

For example, in case of the TE surface mode incidence from one side, the reflection coefficient R_{total}, the transmission coefficient T_{total}, and the coupling coefficients $C_{R\text{total}}$ and $C_{T\text{total}}$ to the TM mode can be obtained as follows:

$$
\begin{aligned}
R_{\text{total}} &= \frac{\tau_{21}\tau_{33} - \tau_{23}\tau_{31}}{\Delta\tau} \\
T_{\text{total}} &= \frac{\tau_{33}}{\Delta\tau} \\
C_{R\text{total}} &= \frac{\tau_{41}\tau_{33} - \tau_{43} - \tau_{31}}{\Delta\tau} \\
C_{T\text{total}} &= -\frac{\tau_{31}}{\Delta\tau} \qquad (\Delta\tau = \tau_{11}\tau_{33} - \tau_{13}\tau_{31})
\end{aligned} \tag{12}
$$

where τ_{mn} is an element of the transmission matrix $\boldsymbol{T}_{\text{total}}$.

On the other hand, the infinite periodic corrugation can be regarded as an infinitely cascaded connection of the unit cell as described before. Then the transmission characteristics of infinite periodic corrugation can be obtained by applying the Floquet's theorem to a unit cell and by solving the following eigenvalue equation:

$$
|\boldsymbol{T}_{\text{unit}}^n - e^{-\Gamma d}\mathbf{1}| = 0
$$

where $\Gamma = \alpha + j\beta$ is the propagation constant to be solved, d is the period of the corrugation, and $\mathbf{1}$ means the unit

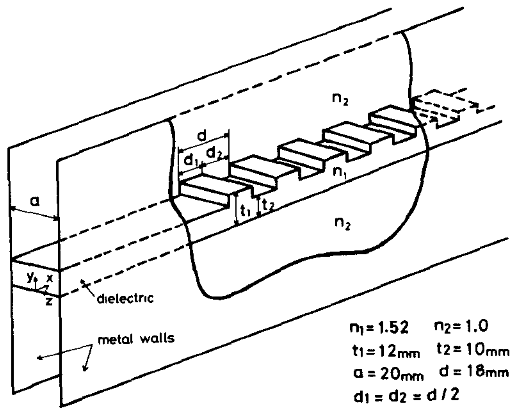

Fig. 4. H-guide with finite periodic corrugation.

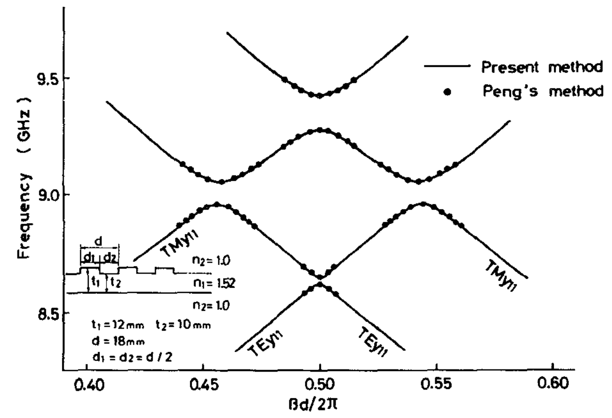

Fig. 5. Dispersion characteristics of the H-guide with infinite periodic corrugation in the Bragg interaction region.

matrix. This approach will be compared numerically with an alternative one presented by Peng [17].

C. H-Guide Having a Periodic Corrugation

We have discussed so far the oblique incident problem for the corrugated dielectric slab waveguide. Such a problem is applied to a structure easily prepared at X-band, i.e., the corrugated H-guide shown in Fig. 4. If the metal wall separation a of the H-guide is properly chosen, each building block with uniform thickness t_1 or t_2 can support TE_{y11}, TM_{y11}, and TE_{y01} modes.[1] In this case, the wavenumber k_z in the z direction is fixed to π/a for the first two modes, while k_z of the TE_{y01} mode is equal to zero. The situation given by $k_z \neq 0$ can be identified with the oblique incidence of the surface wave to the discontinuity at the angle θ which is given by $\theta = \sin^{-1}(k_z/k_s) = \sin^{-1}(\pi/k_s a)$. Therefore, there is necessary coupling between TE_{y11} and TM_{y11} modes.

On the other hand, these modes are orthogonal to the TE_{y01} mode in a functional sense over the yz cross section. So, the corrugated H-guide will be numerically and experimentally investigated by considering only TE_{y11} and TM_{y11} modes in the following sections.

III. Numerical Results

Before discussing the accuracy of our analytical approach by scaled experiments in the 10-GHz region, numerical discussions are first presented in this section. Fig. 4 shows the construction of the corrugated H-guide which consists of both a polyethylene ($n_1 = 1.52$) as a dielectric and copper plates as the metal walls. The thicknesses of the polyethylene are chosen to be $t_1 = 12$ mm and $t_2 = 10$ mm, and the wall separation is chosen to be $a = 20$ mm. The period of the corrugation is chosen to be $d_1 = d_2 = d/2 = 9$ mm so that the stopbands corresponding to the Bragg reflection occur in the 10-GHz region. For this structure, the H-guide having uniform thickness t_1 or t_2 can support three modes, i.e., TE_{y01}, TE_{y11}, and TM_{y11} modes. As described in the previous section, it is sufficient to take only TE_{y11} and TM_{y11} modes into account in the analysis.

[1] TE_{ypq} (TM_{ypq}) mode denotes TE (TM) mode with respect to the y direction, and the subscript p relates to $p\pi/a$, while q indicates the number of extrema of E_y (H_y) component in the y direction.

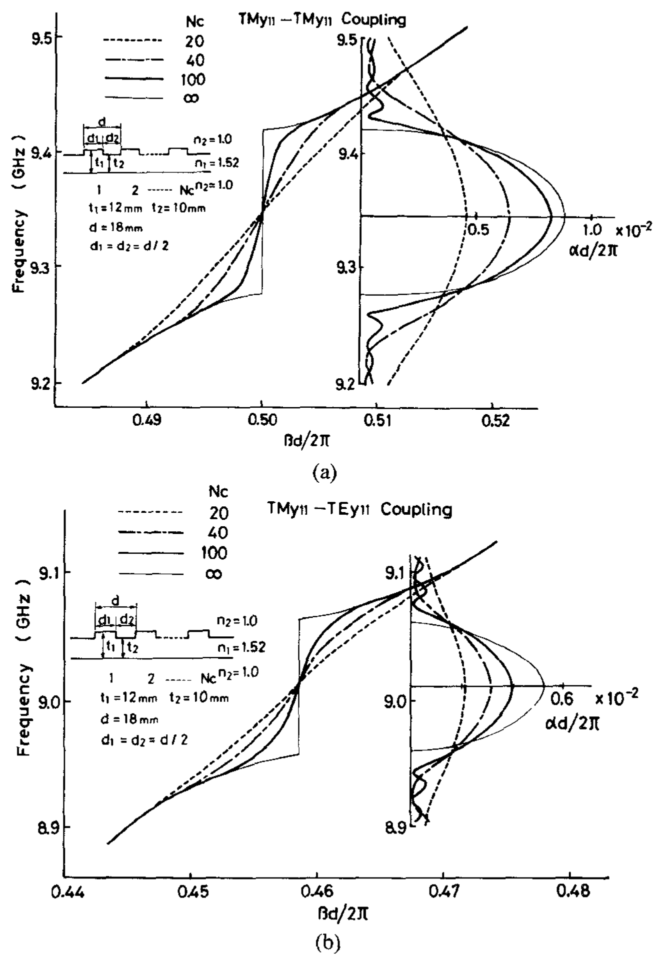

Fig. 6. Phase and attenuation constants of the H-guide with finite periodic corrugation around (a) TM_{y11}–TE_{y11} and (b) TM_{y11}–TM_{y11} coupling regions.

Fig. 5 shows a portion of the dispersion curve calculated from (13) for the H-guide with the infinite periodic corrugation. These curves denoted in the

$$\frac{\omega}{2\pi} - \frac{\beta d}{2\pi}$$

form are limited in the first stopband region. It is seen that

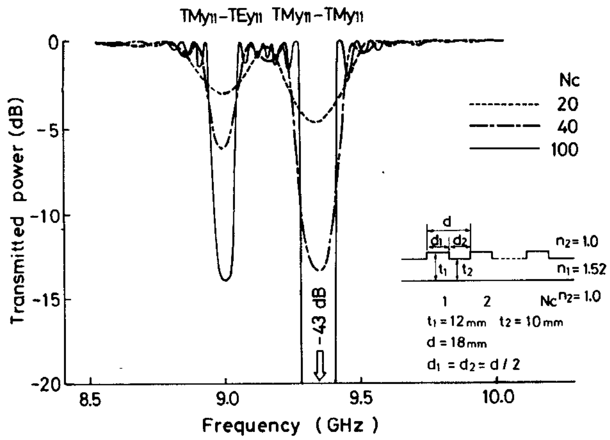

Fig. 7. Frequency characteristics of transmitted power of the TM_{y11} mode for the finite periodic case.

four stopbands appear here, one due to TE_{y11}–TE_{y11} coupling, another due to TM_{y11}–TM_{y11} coupling, and two others due to coupling between TE_{y11} and TM_{y11} modes. It is confirmed that these calculated results agree well with the results of Peng's method indicated with dots, so we can recognize that the transmission matrix of a unit cell of the periodic corrugation is successfully obtained by the present method. Using this transmission matrix, the propagation characteristics for the finite periodic case can be calculated from its cascaded connection, and the typical results calculated for TM_{y11}–TM_{y11} coupling and also for TM_{y11}–TE_{y11} coupling regions are shown in Fig. 6(a) and (b), where the number of unit cell N_c is a parameter. These figures show clearly the effect of N_c on the propagation characteristics, which approach those for infinite periodic corrugation, i.e., $N_c = \infty$ with N_c increasing. From these results, the characteristics of transmitted power of the TM_{y11} mode can be easily obtained and are shown in Fig. 7. It is found from this figure that both TM_{y11}–TE_{y11} and TM_{y11}–TM_{y11} couplings in case of $N_c = 20$ have weak effects on the propagation characteristics of the TM_{y11} mode, while the coupling in case of $N_c = 100$ becomes so strong that the two distinct stopbands appear.

IV. Experiments

A. Experimental Setup

The experimental setup for measuring the transmission and the reflection characteristics in the 10-GHz region is shown schematically in Fig. 8(a), where the construction of the H-guide tested is the same as that described in Section III. In this setup, the H-guide is 40 cm wide and 250 cm long, and the corrugation is located at the center of the guide. The power from the microwave oscillator is launched into an H-guide through a mode launcher which excites the TM_{y11} mode.

The transmission characteristics of the TM_{y11} mode can be obtained by measuring the ratio of the output power of the H-guide with a corrugation to that without it. Also, the reflection characteristics of the TM_{y11} mode can be obtained by measuring the ratio of the reflected power of the corrugated H-guide terminated with a matched load to that

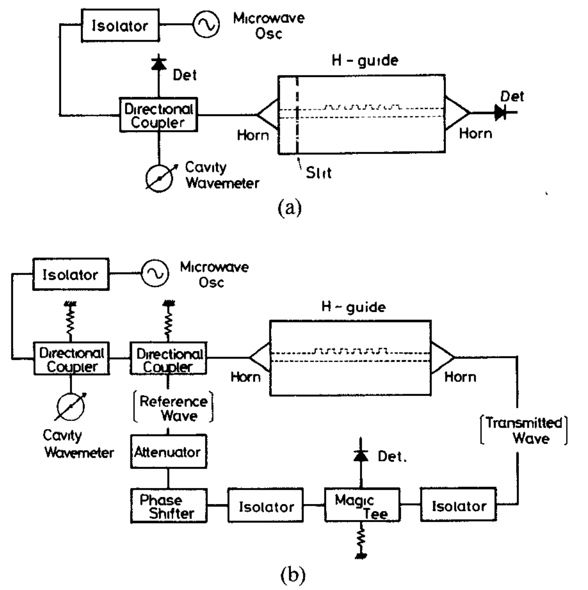

Fig. 8. Schematic diagram of the experimental setups for (a) measurements of transmitted and reflected powers and for (b) measurement of the phase constant (the slit shown in (a) is used to measure the reflected power of TE_{y11} mode).

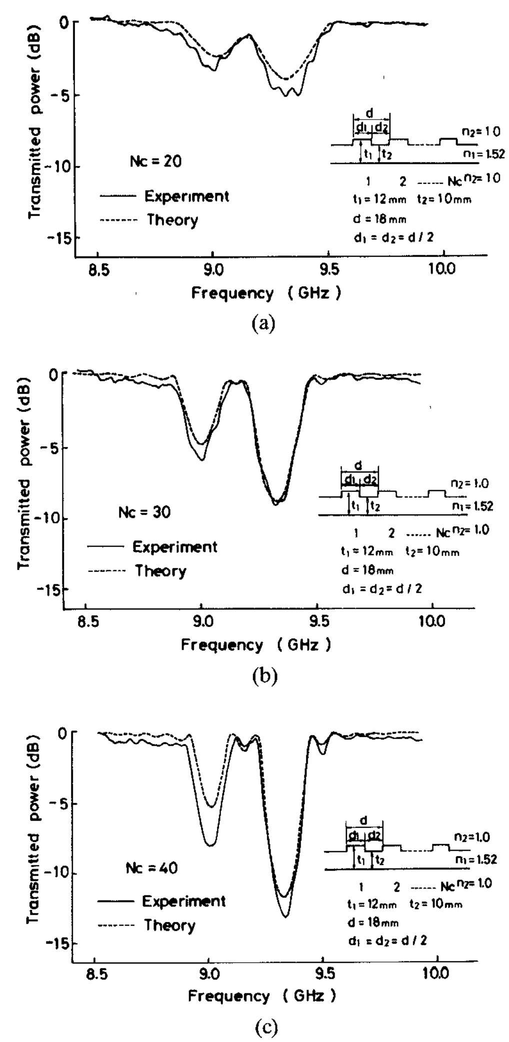

Fig. 9. Measured transmission characteristics of the TM_{y11} mode for (a) $N_c = 20$, (b) $N_c = 30$, and (c) $N_c = 40$. Two stopbands appear at around 9 and 9.35 GHz.

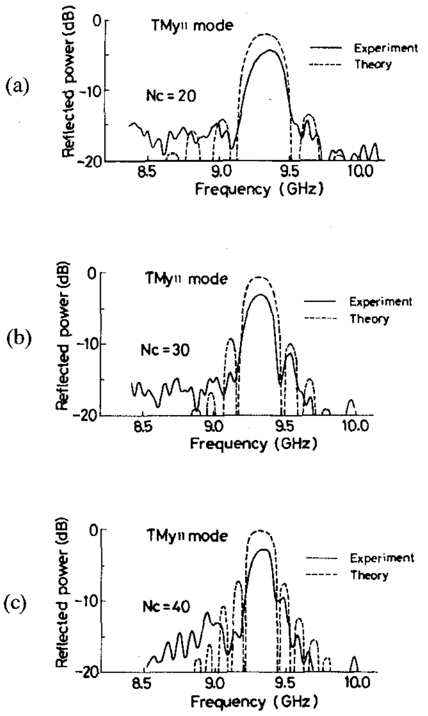

Fig. 10. Measured reflection characteristics of the TM_{y11} mode for (a) $N_c = 20$, (b) $N_c = 30$, and (c) $N_c = 40$. The reflection peak occurs at around 9.35 GHz.

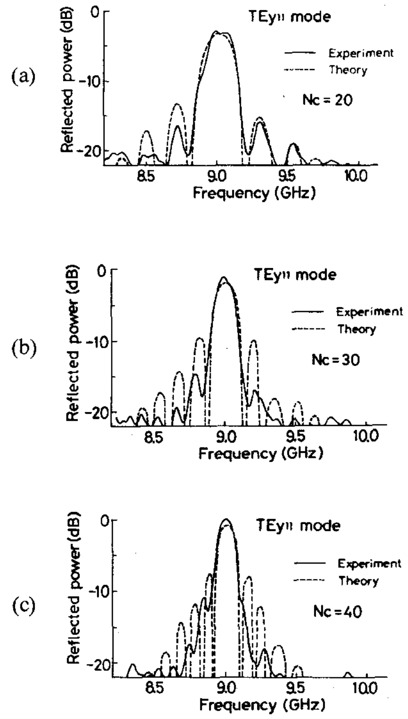

Fig. 11. Measured reflection characteristics of the TE_{y11} mode for (a) $N_c = 20$, (b) $N_c = 30$, and (c) $N_c = 40$. The reflection peak occurs at around 9 GHz.

of the uncorrugated H-guide terminated with a short circuit. However, when it is necessary to measure the reflected power of the TE_{y11} mode, the method mentioned above cannot be followed because the polarization converted TE_{y11} mode is not detected through the TM_{y11}-mode launcher. Therefore, we prepared a 1-mm slit on one of the copper plates at the position near the launching horn, perpendicular to the propagation direction of an H-guide, and a small pyramidal horn antenna was used to measure the relative power of reflected TE_{y11} mode radiated in space. As easily understood, the wall current of the TM_{y11} mode has no component along the propagation direction, so that the incident TM_{y11} mode can propagate without the influence of a slit, and only the reflected TE_{y11} mode can selectively radiate from the slit.

On the other hand, the measurement of the phase constant of the TM_{y11} mode is performed by the experimental setup shown in Fig. 8(b). The phase constant can be obtained from the difference of the phase shifts between the corrugated and the uncorrugated H-guides.

B. Experimental Results

Fig. 9(a), (b), and (c) shows the characteristics of transmitted power of the incident TM_{y11} mode for $N_c = 20$, 30, and 40, respectively, where the solid lines indicate the measured values and the dashed lines indicate the theoretical ones by the present method. From these figures, we can observe two stopbands in this frequency region, and all of these cases show the good agreement between the theoretical and the experimental values. The center frequencies at two stopbands are very accurately predicted, whereas their dips are slightly different between both values. This small discrepancy may be caused by the influence due to the

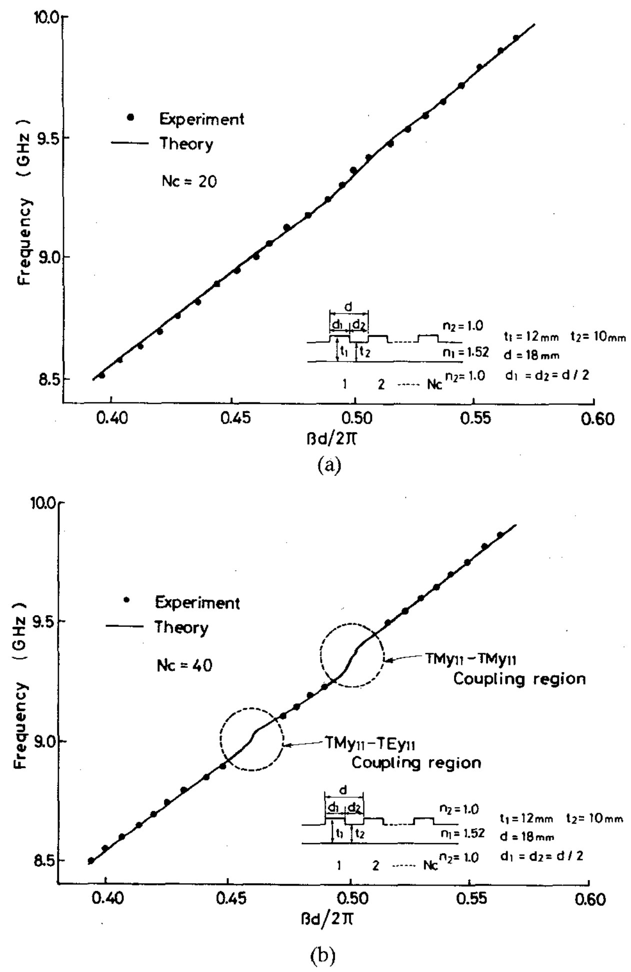

Fig. 12. Measured phase constants of the TM_{y11} mode for (a) $N_c = 20$ and (b) $N_c = 40$ (the enlargement of coupling regions is shown in Fig. 13).

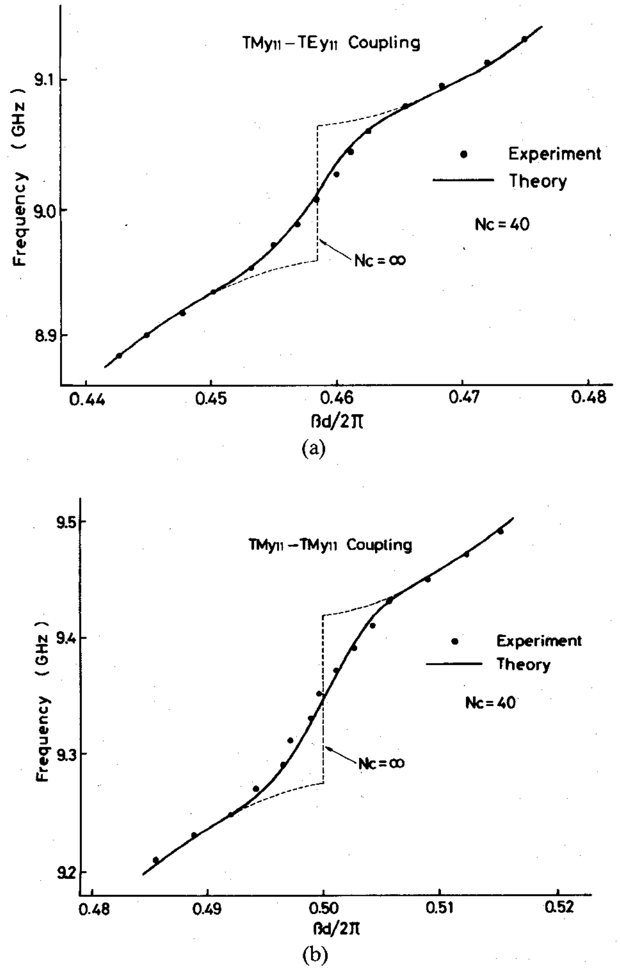

Fig. 13. Measured phase constants of the TM_{y11} mode around (a) the TM_{y11}–TE_{y11} and (b) the TM_{y11}–TM_{y11} coupling regions (in case of $N_c = 40$).

neglected radiation field which occurs at the corrugations.

Although it is obvious from the theoretical prediction that the measured stopbands at 9.01 GHz and 9.35 GHz are identified with the TM_{y11}–TE_{y11} coupling and TM_{y11}–TM_{y11} coupling, respectively, we shall next confirm experimentally their couplings by measuring the reflected power of each type of modes. Fig. 10(a), (b), and (c) shows the characteristics of reflected power on the incident TM_{y11} mode for $N_c = 20$, 30, and 40, where the solid lines indicate the measured values and the dashed lines indicate the theoretical ones. On the other hand, Fig. 11(a), (b), and (c) shows the characteristics of relative power of the reflected TE_{y11} mode for $N_c = 20$, 30, and 40. In these figures, the maximum value of the relative power measured for $N_c = 20$ is normalized so as to coincide with that of the theoretical one indicated by the dashed line. Now, overlapping these reflection characteristics on the transmission ones of Fig. 9, it is clearly proven that the stopband around 9 GHz is caused by TM_{y11}–TE_{y11} coupling, while that around 9.35 GHz is caused by TM_{y11}–TM_{y11} coupling.

Finally, Fig. 12(a) and (b) shows the measured phase constants of the TM_{y11} mode for $N_c = 20$ and 40. Especially, the enlargements around two coupling regions are depicted in Fig. 13(a) and (b) for $N_c = 40$. It is clear that the measured values for the finite periodic case are found to be different from the dispersion characteristics for the infinite periodic case indicated by the dashed line, and show a fairly good agreement with the solid line calculated by the present method.

V. Conclusion

The analytical method for an open dielectric waveguide with the finite periodic corrugation is presented. In this approximate method, the step discontinuity in a planar dielectric waveguide is expressed by a transmission matrix for waves guided obliquely to the discontinuity, and the finite periodic corrugation is regarded as its cascaded connection. Although the analysis is roughly approximated by treating only a surface wave mode and by neglecting radiation waves, the calculated results sufficiently explain the experimental ones of the propagation characteristics at the stopbands due to the Bragg reflection. The present method will become one of straightforward and effective methods for investigating the propagation characteristics of an open dielectric waveguide with finite periodic corrugation.

References

[1] C. Elachi, "Waves in active and passive periodic structure: A review," *Proc. IEEE*, vol. 64, pp. 1666–1698, Dec. 1976.
[2] D. Marcuse, *Theory of Dielectric Optical Waveguides*. New York: Academic, 1974, ch. 3.
[3] W. Streifer, D. R. Scifres, and R. D. Burham, "Coupled wave analysis of DFB and DBR lasers," *IEEE J. Quantum Electron.*, vol. QE-13, pp. 134–141, Apr. 1977.
[4] A. Yariv, "Coupled-mode theory for guided-wave optics," *IEEE J. Quantum Electron.*, vol. QE-9, pp. 919–933, Sept. 1973.
[5] Y. Yamamoto, T. Kamiya, and H. Yanai, "Improved coupled mode analysis of corrugated waveguides and lasers," *IEEE J. Quantum Electron.*, vol. QE-14, pp. 245–258, Apr. 1978.
[6] S. T. Peng, H. L. Bertoni, and T. Tamir, "Analysis of periodic thin-film structures with rectangular profiles," *Opt. Commun.*, vol. 10, pp. 91–94, Jan. 1974.
[7] S. T. Peng, T. Tamir, and H. L. Bertoni, "Theory of periodic dielectric waveguides," *IEEE Trans. Microwave Theory Tech.*, vol. MTT-23, pp. 123–133, Jan. 1975.
[8] T. E. Rozzi, "Rigorous analysis of the step discontinuity in a planar dielectric waveguide," *IEEE Trans. Microwave Theory Tech.*, vol. MTT-26, pp. 738–746, Oct. 1978.
[9] T. E. Rozzi and G. H. In'tveld, "Field and network analysis of interacting step discontinuities in planar dielectric waveguides," *IEEE Trans Microwave Theory Tech.*, vol. MTT-27, pp. 303–309, Apr. 1979.
[10] H. M. Stoll, "Distributed Bragg deflector: A multifunctional integrated optical devices," *Appl. Opt.*, vol. 17, pp. 2562–2569, Aug. 1978.
[11] A. C. Livanos, A. Katzir, A. Yariv, and C. S. Hong, "Chirped-grating demultiplexers in dielectric waveguides," *Appl. Phys. Lett.*, vol. 30, pp. 519–521, May 1977.
[12] J. P. Hsu, S. T. Peng, and A. A. Oliner, "Scattering by dielectric step discontinuities for obliquely incident surface waves," in *Dig. URSI Meeting*, (College Park, MD), May 1978, p. 46.
[13] K. Wagatsuma, H. Sakaki, and S. Saito, "Mode conversion and optical filtering of obliquely incident waves in corrugated waveguide filters," *IEEE J. Quantum Electron.*, vol. QE-15, pp. 632–637, July 1979.
[14] M. J. Shiao, H. Shigesawa, S. T. Peng, and A. A. Oliner, "Mode conversion effects in Bragg reflection from periodic grooves in rectangular dielectric image guide," in *1981 IEEE MTT-S Microwave Symp. Dig.*, (Los Angeles, CA), June 1981, pp. 14–16.
[15] S. T. Peng and A. A. Oliner, "Guidance and leakage properties of a class of open dielectric waveguides: Part 1—Mathematical formulations," *IEEE Trans. Microwave Theory Tech.*, vol. MTT-29, pp. 843–855, Sept. 1981.
[16] D. Marcuse, *Light Transmission Optics*. Van Nostrand, 1972, ch. 8.3.

[17] S. T. Peng, "Oblique guidance of surface waves on corrugated dielectric layers," in *Proc. Int. URSI Symp. Electromagnetic Waves*, Aug. 1980, paper no. 341B.

Mikio Tsuji (S'77–M'82) was born in Kyoto, Japan, on September 10, 1953. He received the B.S. and M.S. degrees in electrical engineering from Doshisha University, Kyoto, Japan, in 1976 and 1978, respectively.

Since 1981, he has been a Research Assistant of the Faculty of Engineering at Doshisha University. His research activities have been concerned with submillimeter-wave and microwave transmission lines and devices of open structures.

Mr. Tsuji is a member of the Institute of Electronics and Communication Engineers (IECE) of Japan.

Soichi Matsumoto (S'81) was born in Osaka, Japan, on March 22, 1959. He received the B.S. and M.S. degrees in electrical engineering from Doshisha University, Kyoto, Japan, in 1981 and 1983, respectively. He is now with the Mitsubishi Electrical Corporation.

Mr. Matsumoto is a member of the Institute of Electronics and Communication Engineers (IECE) of Japan.

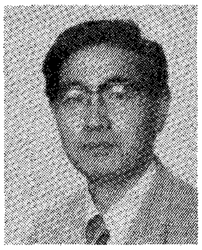

Hiroshi Shigesawa (S'62–M'63) was born in Hyogo, Japan, on January 5, 1939. He received the B.S., M.S., and Ph.D. degrees in electrical engineering from Doshisha University, Kyoto, Japan, in 1961, 1963, and 1969, respectively.

Since 1963, he has been with Doshisha University. From 1979 to 1980, he was a Visiting Scholar at the Microwave Research Institute, Polytechnic Institute of New York, Brooklyn, NY. Currently, he is a Professor at the Faculty of Engineering, Doshisha University. His present research activities involve microwave and submillimeter-wave transmission lines and devices of open structure, fiber optics, and scattering problems of electromagnetic waves.

Dr. Shigesawa is a member of the Institute of Electronics and Communication Engineers (IECE) of Japan, the Japan Society of Applied Physics, and the Optical Society of America (OSA).

Kei Takiyama (M'58) was born in Osaka, Japan, on October 20, 1920. He received the B.S. and Ph.D. degrees in electrical engineering from Kyoto University, Kyoto, Japan, in 1942 and 1955, respectively.

Since 1954, he has been a Professor of Electronic Engineering at Doshisha University, Kyoto, Japan, where he carried out research in the fields of microwave transmission lines and optical engineering. From 1957 to 1958, he was a Fulbright Scholar and a Research Associate at the Microwave Research Institute, Polytechnic Institute of Brooklyn, NY.

Dr. Takiyama is a member of the Institute of Electronics and Communication Engineers (IECE) of Japan, the Institute of Electrical Engineers of Japan, and the Optical Society of America (OSA).

Hybrid Modes in Circular Cylindrical Optical Fibers

KATSUMI MORISHITA, MEMBER, IEEE

Abstract—**The classification of hybrid modes in circular cylindrical optical fibers is studied. It is shown that problems of the mode classifications, i.e., the crossover of the dispersion characteristics and the remarkable changes of the polarization states and the field configurations, are caused by the coupling of the HE-type and EH-type modes.**

I. Introduction

RECENTLY, various optical fibers, including multimode fibers, single-mode fibers, single polarization fibers, and dual-mode fibers, have been produced. In general, propagation modes supported by multimode fibers are called linearly polarized (LP) "modes" [1], which are not true modes. In case the optical fibers have few propagation modes, the difference between the corresponding true modes for each LP "mode" is of practical importance for calculating fiber bandwidths and designing fibers [2]. The descriptive names TE, TM, HE, and EH are usually used for distinguishing propagation modes. There are several classifications of hybrid modes, which are based on the amplitude coefficient ratio of axial components of electric and magnetic fields [3], [4], the polarization states [5], [6] and the field configurations [7] of propagation modes, and the factorization of characteristic equations [8], [9].

Manuscript received July 22, 1982; revised December 8, 1982.
K. Morishita is with the Department of Precision Engineering, Osaka Electro-Communication University, Neyagawa, Osaka 572, Japan.